Supporting information for "Understanding of Deformation Mechanism and Mechanical Characteristics of Cementitious Mineral analogues From First Principles and Reactive Force Field Molecular Dynamics"

Jinyang Jiang[a], Yiru Yan[b], Dongshuai Hou[c]*, Jiao Yu[d]

a. Professor, Southeast University, Nanjing, China, jiangjinyang16@163.com;
b. PhD, Southeast University, Nanjing, China, yiruyan@seu.edu.cn;
c. Corresponding author, Professor, Qingdao University of Technology, Qingdao, China, email: dshou@outlook.com.
d. PhD, Qingdao University of Technology, Qingdao, China, email:yujiaoa@126.com

S1. Validation of the MD model by reactive force field

The crystal parameter and mechanical properties calculated by the reactive force field MD have been compared with the DFT results and listed in the Table S1 and Table S2, respectively. As listed in Table S1, the cell parameters for three types of crystal are calculated after the geometry optimization by the reactive force field. It matches well with the DFT data, indicating the accuracy of the force field in describing the structural properties of the C-S-H crystal. The initial ordered crystal structure, described by the reactive force field, determines the accuracy for the subsequently mechanical study. On the other hand, the Young's modulus of Jennite and Tobermorite crystal along x, y and z directions are obtained by linearly fitting the elastic regime of the corresponding stress-strain curves. As compared with DFT results, the Young's modulus obtained from the uniaxial tensile test by ReaxFF MD is overestimated (around 5% to 13%).

Table S1. Crystal cell parameters for Jennite, Tobermorite 9 and Tobermorite 11 crystal calculated by the Reactive force field Method, DFT method and experimental results.

	C/S	a (Å)	b (Å)	c(Å)	α(°)	β (°)	γ(°)

|	Method		a	b	c	α	β	γ
Jennite	Exp.[7]	1.5	10.52	7.25	10.92	101.4	96.90	109.40
	ReaxFF		10.23	7.16	11.09	101.09	96.72	108.58
	GGA+vdW		10.55	7.25	10.86	101.17	97.44	109.47
Tobermotire 9 Å	Exp.[21]	0.83	11.16	7.30	9.57	101.08	92.83	89.98
	ReaxFF		10.90	7.61	9.49	103.19	92.05	89.55
	GGA+vdW		11.22	7.35	9.61	101.63	92.23	90.34
Tobermotire 11 Å	Exp.[8]	0.66	6.74	7.39	22.49	90.00	90.00	123.25
	ReaxFF		6.70	7.55	22.85	90.00	90.00	123.25
	GGA+vdW		6.79	7.44	22.60	90.00	90.00	123.63

Table S2. Young's Modulus along x, y and z direction for Jennite, Tobermorite 9 Å and Tobermorite 11 Å crystal calculated by the Reactive force field Method and DFT method (units: GPa)

|	Method	E_x	E_y	E_z
Jennite	ReaxFF MD	75.80	85.19	42.29
	DFT	80.50	96.46	32.09
Tobermorite 9	ReaxFF MD	137.97	133.67	140.14
	DFT	131.16	129.80	125.88
Tobermorite 11	ReaxFF MD	73.98	105.14	131.43
	DFT	98.88	91.92	120.56

S2. The loading rate influence on the mechanical properties of C-S-H crystals

In order to study the influence of the tensile strain rate on the mechanical behavior of the C-S-H crystals, molecular dynamics was utilized to model the uniaxial tensile test on the tobermorite 9 Å, tobermorite 11 Å and Jennite crystals along x, y and z directions with strain rate of 0.008/ps, 0.04/ps and 0.08/ps. Take the tensioned tobermorite 9 Å crystal for example. In the elastic region, the stress-strain curves exhibit almost no differences at different loading rate. It means that the tensile rate varying in current range has little influence the Young's modulus of the C-S-H crystal. As shown in Figure S1, the strength and failure strain are reduced to some extent with decreasing loading rate for the tobermorite crystal tensioned along x direction. In the post-failure region, the stress drops earlier for the tobermorite tensioned with slower loading rate. It can be observed in Figure S2 that after the elastic regime, the stress first reduces slightly and

then increases to some extent, which is defined as the "strain hardening" stage in the manuscript. With decreasing of the loading rate, the strength enhancement is reduced in the strain hardening stage. The strength weakening in the "strain hardening" stage in the slow loading rate can also be observed in Figure S2b and Figure S3b for the tensioned tobermorite 11 Å and Jennite crystals. Additionally, as shown in Figure S1c, when the crystal is tensioned along z direction, the structure is more likely to be stretched broken due to the weak interlayer bonding. With decreasing loading rate, the fracture strain of the tensioned structure reduces from 0.8 to 0.4. This can be explained by that at slow loading rate, the crack has enough time to develop across the entire crystal structure, resulting in the fracture of the crystal. Therefore, the strength and strain at failure are positively related to the loading rate. In the tensile process, when the strain flows from the high density region to the low density region, the atomic movements directly results in the coalescence of the defections in the molecular structure. The small loading rate provides sufficient time for the atomic rearrangement such as the bond stretching and angle opening. It results in the growth of the crack in the crystal and earlier failure for the layered structure.
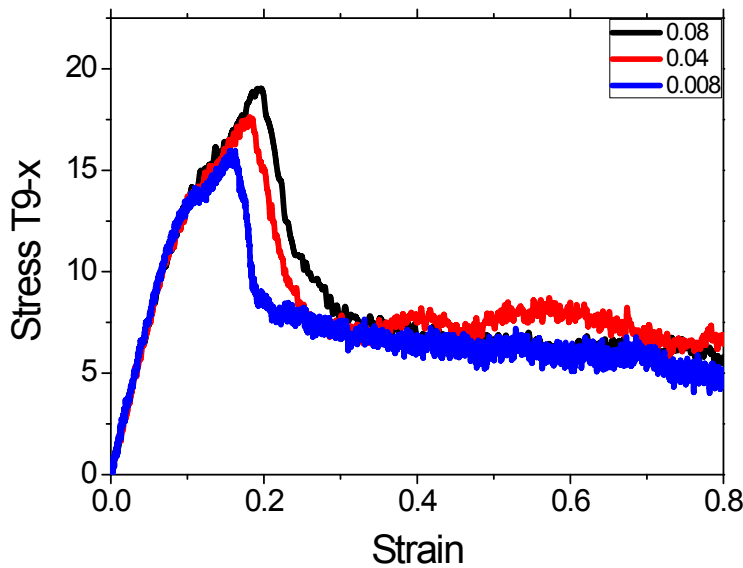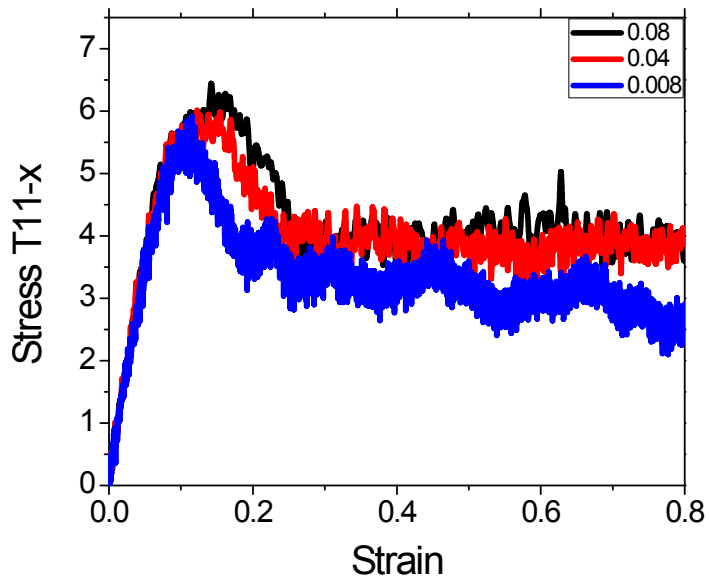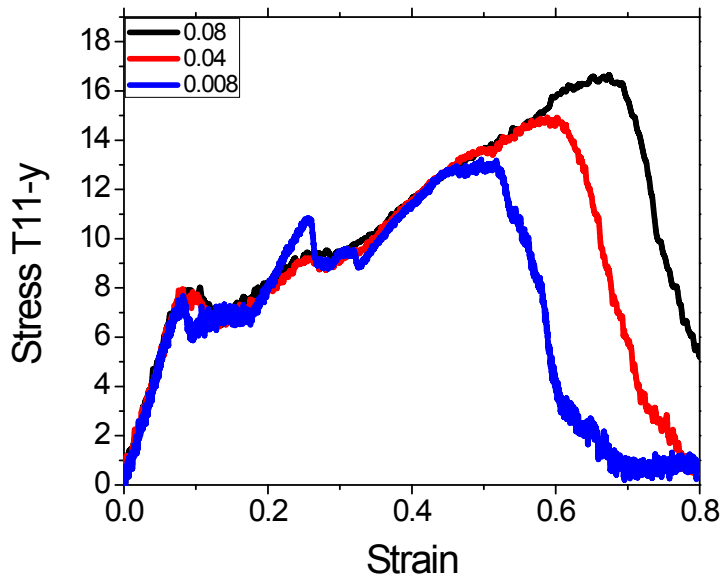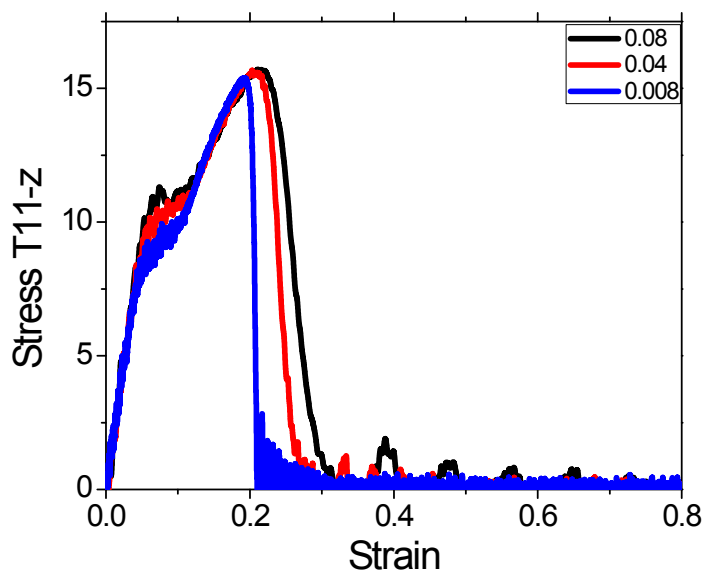

(a)
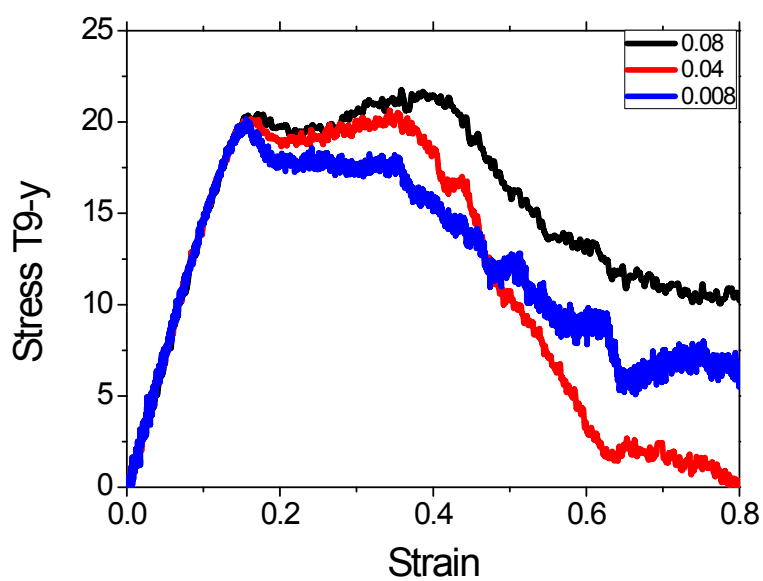
(b)
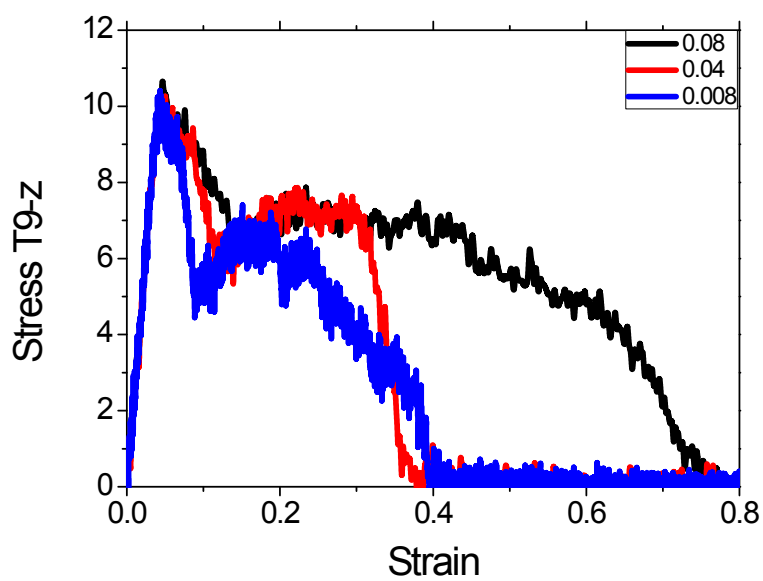
(c)

Figure S1 Stress-strain relation for tobermorite 9Å tensioned along (a) x, (b) y and (c) z direction

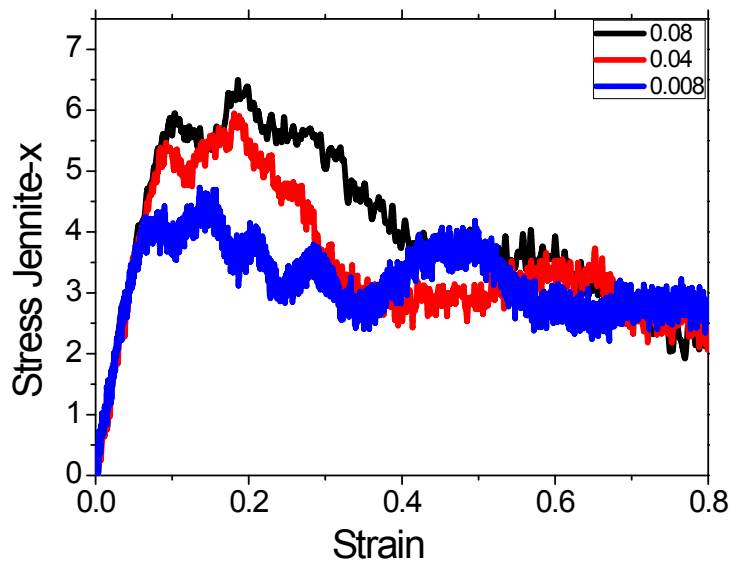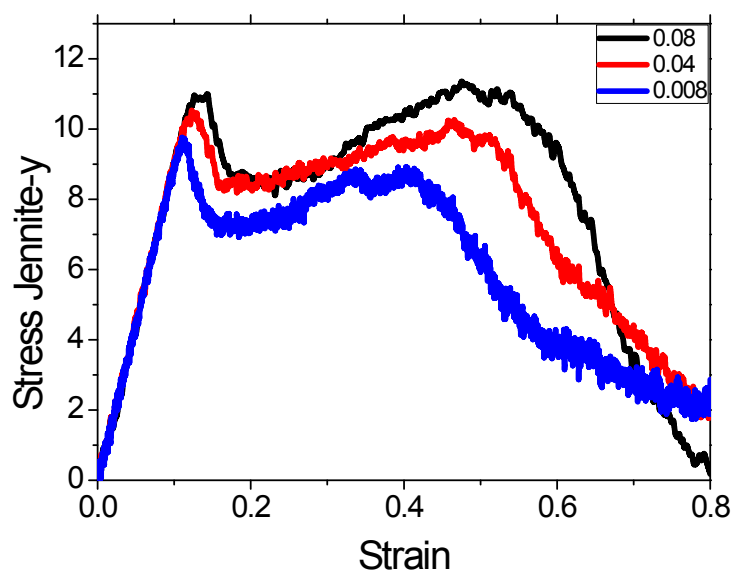with tensile strain of 0.08/ps, 0.04/ps and 0.008/ps
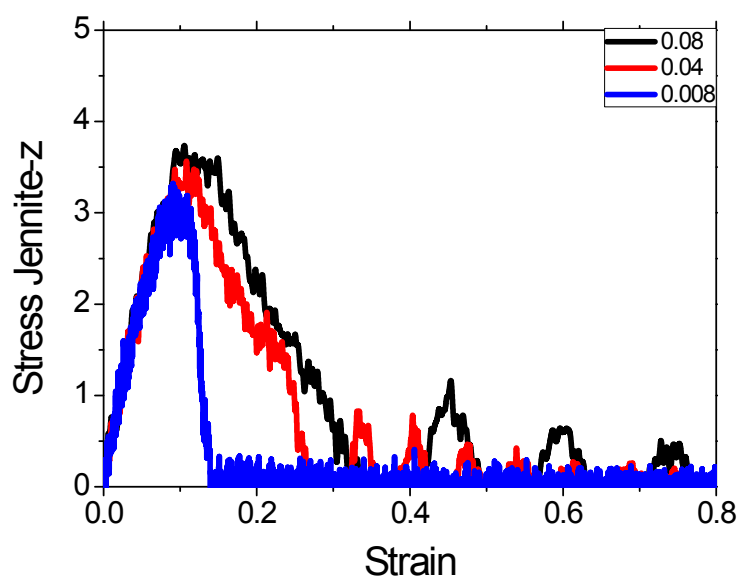
(a)

(b)

(c)

Figure S2 Stress-strain relation for tobermorite 11Å tensioned along (a) x, (b) y and (c) z direction

with tensile strain of 0.08/ps, 0.04/ps and 0.008/ps

(a)

(b)

(c)

Figure S3 Stress-strain relation for Jennite tensioned along (a) x, (b) y and (c) z direction with

tensile strain of 0.08/ps, 0.04/ps and 0.008/ps

S3. Dynamic properties of the H atoms and hydrolytic reaction

The dynamic properties of the H atoms in the three crystals during the tensile process are

calculated by the mean square displacement (MSD), as defined in the following equation.

$$MSD(t) = \langle |r_i(t) - r_i(0)|^2 \rangle \qquad \text{(S1)}$$

The MSD value oscillation with time t describes the average square of the displacement that the atoms at time t deviate from their original positions. As shown in Figure S4, the MSD for H atoms progressively rises in the tensioned tobermorite and jennite crystal during 100 ps. The MSD remains constant during the first 10 ps. It means that in the elastic regime, the water molecules are ultra-confined in the interlayer region and show quite low mobility. Afterward, the MSD of H atoms continues increasing. On the one hand, the layered structure is tensioned broken, producing plenty of defective region where water molecules freely diffuse. On the other hand, the damage silicate chains show high reactivity, accelerating the dissociation of water molecules.
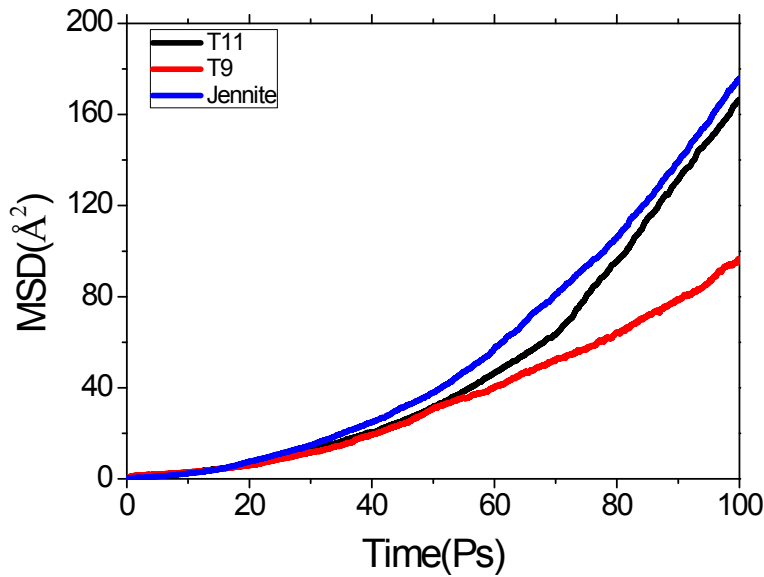

Figure S4. MSD of the H atoms in the Jennite and tobermorite crystals tensioned along y directions

Additionally, the dynamic hydrolytic reaction is characterized by the hydrolytic reaction degree as the function of simulation time, as shown in Figure S5. No hydrolytic reaction happens during the first 50 ps, which is corresponding to the elastic regime and "strain hardening" regime in the stress-strain relation. Subsequently, the hydrolytic reaction degree rapidly increases to nearly 23% during the late 50 ps, where cracks develop and fracture widely happens

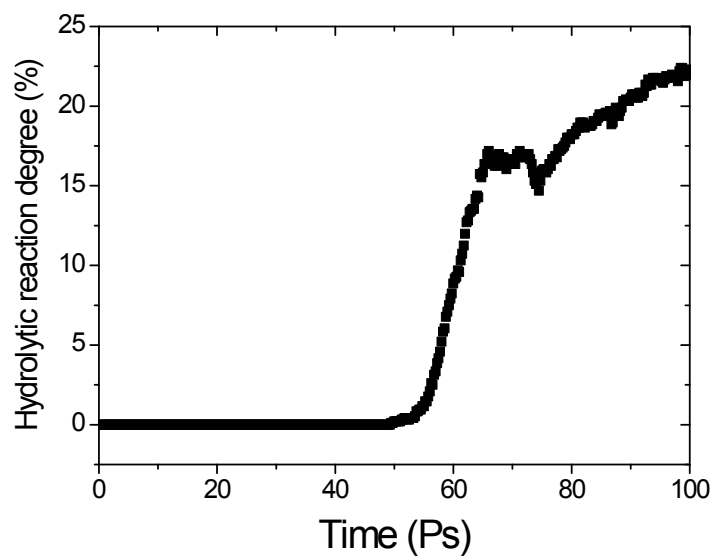in the damaged tobermorite structure.

Figure S4. The evolution of hydrolytic reaction degree of water molecules confined in tobermorite 11 Å tensioned along y direction.